New Journal of Physics
The open-access journal for physics

Chemical sputtering of Be due to D bombardment

C Björkas[1,3], K Vörtler[1], K Nordlund[1], D Nishijima[2] and R Doerner[2]

[1] Association Euratom/Tekes, Department of Physics, University of Helsinki, PO Box 43, FI-00014, Finland
[2] Center for Energy Research, University of California at San Diego, La Jolla, CA 92093, USA
E-mail: carolina.bjorkas@helsinki.fi

New Journal of Physics **11** (2009) 123017 (12pp)
Received 26 August 2009
Published 16 December 2009
Online at http://www.njp.org/
doi:10.1088/1367-2630/11/12/123017

Abstract. While covalently bonded materials such as carbon are well known to be eroded by chemical sputtering when exposed to plasmas or low-energy ion irradiation, pure metals have been believed to sputter only physically. The erosion of Be when subject to D bombardment was in this work measured at the PISCES-B facility and modelled with molecular dynamics simulations. During the experiments, a chemical effect was observed, since a fraction of the eroded Be was in the form of BeD molecules. This fraction decreased with increasing ion energy. The same trend was seen in the simulations and was explained by the swift chemical sputtering mechanism, showing that pure metals can, indeed, be sputtered chemically. D ions of only 7 eV can erode Be through this mechanism.

Contents

[3] Author to whom any correspondence should be addressed.

1. Introduction

The sputtering of materials by energetic particle bombardment is of major theoretical [1]–[4] and practical [5]–[7] interest. Sputtering can occur by many different mechanisms. While physical sputtering from linear cascades, i.e. atom ejection due to a sequence of ballistic collisions between atoms, is well understood [1, 2], other types of sputtering such as that from heat spikes [8] or due to chemical effects [9, 10] are still subject to scientific scrutiny. Although chemical sputtering by low-energy ions is important for plasma processing of materials [11] and the development of fusion reactors [12, 13], it is poorly understood because of difficulties of running controlled experiments for very low ion energies. Computer simulations and experiments have nevertheless recently established that carbon-based materials can be eroded chemically by a 'swift chemical sputtering' mechanism [14]–[19]. However, chemical sputtering has been believed to be not important in metals [9, 20].

Due to its low Z and oxygen gettering abilities, beryllium has been chosen as first wall armour material for the future fusion reactor ITER [21, 22]. As plasma facing material (PFM), Be will have to withstand not only the plasma heat, but also the bombardment of hydrogen isotopes and other impurities in the plasma. Critical Be-related issues, which are still lacking complete understanding, include formation of mixed materials originating from different PFMs in the reactor and tritium retention [23, 24].

During plasma–wall interaction experiments, BeD molecules have been seen to erode in the JET [25] fusion reactor and in the linear divertor plasma simulator PISCES-B facility [26]–[28], indicating that a chemical sputtering effect is present when Be is subject to deuterium plasma bombardment. Chemical sputtering has not been thoroughly investigated in Be, but the mechanism is nonetheless important and must be taken into account when assessing, for instance, the reactor lifetime, plasma contamination and mixed material formation. The bonding of hydrogen isotopes to Be also increases the tritium retention in the first wall, making the use of tritium removal techniques more crucial.

Using both experimental and computer simulation techniques, this study will focus on the erosion of Be due to a deuterium plasma. Special attention is paid to the chemical sputtering of molecular BeD.

2. Method

2.1. Experimental setup

Experiments were performed at the PISCES-B facility at UCSD. The PISCES devices use a reflex arc style plasma source to generate a steady-state plasma. The plasma density, n_e, and electron temperature, T_e, can be controlled by primarily varying the chamber fill pressure and discharge power [29]. The ion bombarding energy to the targets is obtained by biasing the targets negatively and accelerating the ions through the applied bias potential. This technique provides a fairly monoenergetic energy distribution of ions striking the target surface at normal incidence, since the ion temperature is relatively low ($\sim 0.1T_e$). The errors in the incident ion energy come from uncertainties in the determination of the plasma potential.

During these investigations, Be targets (made of S65C Be from Brush Wellman) were exposed to deuterium plasma and the resultant plasma–material interactions were spectroscopically investigated. The Be targets were clamped onto a water-cooled copper sample holder

allowing the surface temperature to be kept constant at approximately 373 K during the ion bombardment of the target. The parameters of the steady-state plasma were monitored with a double-tip Langmuir probe throughout the duration of the discharge and were $n_e = 2.4 \times 10^{18}\,\mathrm{m}^{-3}$, $T_e = 8\,\mathrm{eV}$ and the ion flux to the target $\Gamma_{ion} \sim 3 \times 10^{22}\,\mathrm{m}^{-2}\,\mathrm{s}^{-1}$. Material eroded from the sample surface was spectroscopically measured using photons emitted from neutral Be atoms at 457.3 nm and from BeD molecules emitted in the A–X band at 497.3–499.2 nm [27]. The photon flux is translated into a particle flux using the photon emission coefficient from the ADAS database [30] (in the case of atomic Be), or the derived photon emission coefficient (for BeD molecules) [27].

A target bias voltage scan was performed while measuring the material eroded as Be atoms and BeD molecules at each bias voltage. The errors in the sputtered particle flux measurements are estimated from variation in the photon emission coefficients due to the error analysis of the Langmuir probe electron temperature, typically ±2 eV.

2.2. Simulation methods

Since erosion is an atomic level mechanism, molecular dynamics (MD) simulations are a suitable tool for studying it. The simulations are, however, limited in time and space which means that exact experimental conditions cannot be reproduced. The fluxes in the simulations are inevitably several orders of magnitudes larger and thermal effects (diffusion and surface relaxations) are also not perfectly modelled due to the short time scales in the simulations. Despite this, simulations are able to give insight into many experimentally observed phenomena.

Here, the deuterium plasma impact on Be was simulated with the MD code PARCAS [31][4] using the recent Be–H potential developed by us [32] (version Be–H I). This potential is of the analytical bond-order type, which was initially developed by Tersoff [33] to describe covalent solids but shown to be extendable to metals [34]–[36] and hydrocarbons [37].

The details and parameters of the potentials are given in [32]. In short, the total energy E of the system is expressed as a sum over individual bond energies, as

$$E = \sum_{i>j} f_{ij}^{c}(r_{ij}) \left[V_{ij}^{R}(r_{ij}) - \underbrace{\frac{b_{ij} + b_{ji}}{2}}_{\overline{b_{ij}}} V_{ij}^{A}(r_{ij}) \right]. \tag{1}$$

f_{ij}^{c} is a cut-off function, making the potentials short ranged, and V_{ij}^{R} and V_{ij}^{A} are the repulsive and attractive terms, respectively. These are pair potentials of a Morse-like form. b_{ij} is the bond-order term, which includes three-body interactions and angularity. The nine adjustable parameters in this formula were fitted to both experimental data and data obtained using density functional theory. In fitting pure Be, properties of several different phases were used and the ground-state structure of Be is well described by the potential. The Be–H potential (which is applicable also to Be–D interactions) was fitted to Be–H molecules and H as interstitial defect in bulk Be.

Both Be (0001) and $(\overline{1}\overline{1}20)$ surfaces were bombarded at normal incidence with deuterium ions, with energies in the fusion relevant range 3–100 eV. Two versions of the surfaces were

[4] The main principles of the MD algorithms are presented in [51, 52]. The adaptive time step and electronic stopping algorithms are the same as in [53].

used, one perfect and one rough. The latter resembles a situation where the surface has been subject to prolonged bombardment, causing a slight surface roughness. This surface was constructed by randomly removing about half of the Be atoms in the first layer of respective surfaces. The average number of neighbours to a surface atom in the rough case was calculated to be 7.24, whereas in the perfect case each surface atom has nine neighbours.

At least 1000 cumulative bombardments, at a flux of about $2.0 \times 10^{28}\,\mathrm{m^{-2}\,s^{-1}}$, were done at each energy. Between every single bombardment, the simulation cell (initially consisting of 3388 Be atoms, size $\sim 30 \times 30 \times 40\,\text{Å}^3$) was shifted randomly in the x- and y-directions so as to model uniform bombardment of the surface. Periodic boundaries in the x- and y-directions were used. The temperature of the borders of the cell was controlled to 320 K during the first 2 ps of the simulation and the two bottommost layers were fixed to mimic an infinite lattice. The temperature of the two layers above the fixed ones was also controlled, but the surface atoms were not affected by the thermostat. The Berendsen temperature scaling was used [38]. After each bombardment, the whole cell was relaxed for 5 ps at 320 K. Electronic stopping [39], included as a frictional force, was applied to atoms with a kinetic energy above 1 eV in the perfect surface cases and 5 eV for the rough surface ones. We use different limits because it came to our knowledge during the course of the simulations that a low limit, ∼1 eV, is, in general, more accurate [40]. However, since the ion energies used here are very low, the difference is not expected to influence the results. No stopping was applied for sputtered atoms nor for D ions before entering the bulk.

The erosion at 100 eV was also simulated using a sample already containing D atoms near the surface. This was realized by first bombarding a perfect (0001) Be cell cumulatively with 1000 10 eV D ions and then using the resulting cell in 100 eV bombardments. The D/Be ratio in the cell was 0.083. This kind of surface could resemble the experimental one, since low-energy neutral atoms and molecules adsorbing on the surface are expected during the measurements.

3. Results and discussion

3.1. Experiments versus simulations

3.1.1. Total sputtering yield. Figure 1 shows both simulated and experimental data for the sputtering yield (D on Be) as a function of incoming D energy. The first and second sets of experimental data are from a review [41], including ion beam experiments that were done at room temperature (set I) and at 600–650 °C (set II). The third and fourth sets are from recent PISCES-B measurements [28], where a plasma flux of $2 \times 10^{22}\,\mathrm{m^{-2}\,s^{-1}}$ was used. Many different samples and temperatures were used in the latter experiment, but here we cite the ones that were done at room temperature using plasma-deposited samples (set III) and at higher temperatures with polycrystalline samples (set IV). The plasma-deposited samples were made by injecting Be atoms into the plasma, creating layers on polycrystalline Be. (For clarity, the uncertainties in set III, about ±10 eV for the energy and ±50% for the yield, are not included in the graph.)

At low energies, the simulated yields agree with the third experimental set. At high energies, agreement with both sets I and III is found, although the experimental scatter is large. At medium (20–50 eV), the simulations agree with sets II and III. The 100 eV value for a pre-bombarded sample is in line with the other simulated 100 eV ones.

Noteworthy is the difference between the values obtained in ion beam devices for samples of different temperatures, sets I and II. As stated in [41], oxide layers are easily formed at the Be

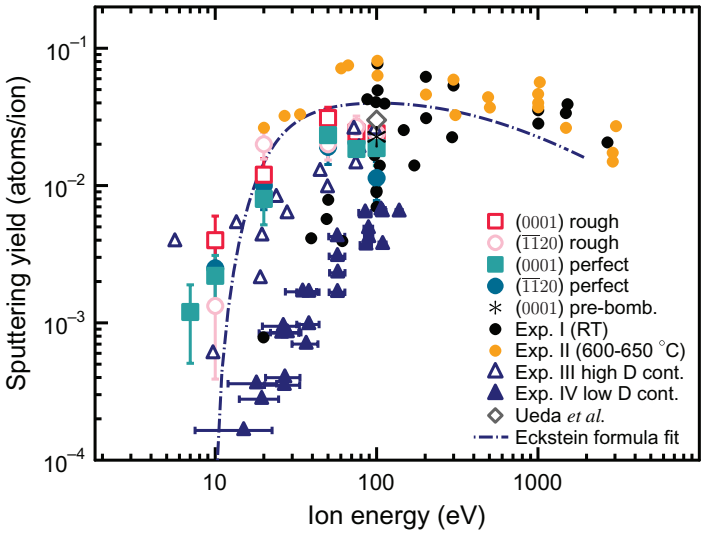

Figure 1. Sputtering yield of D bombardment of Be. The line represents the sputtering formula of Eckstein *et al* [42, 45]. Exp. I and II values are from [41] and Exp. III and IV values are from [28].

surfaces. This increases the surface binding energy and thus lowers the sputtering yield. At high temperatures, however, Be can diffuse through the oxide layer and samples held at 600–650 °C can therefore be considered clean. In the PISCES-B plasma exposure experiments, no oxide layers are expected because the sputtering yield of the oxide is much larger than the amount of oxygen in the plasma [43]. The reason for the method dependency of the sputtering yield (lower yield in plasma experiments than in ion beam ones) is highly unclear. Different D ion fluxes, leading to different D surface saturation rates, and the presence of low-energy neutral D atoms in the plasma could be possible explanations.

Differences are also found when comparing experiments III and IV, which are both done in the same facility. Causing the difference is most likely the amount of D in the sample, since this amount is expected to be higher for the plasma-deposited sample, set III. A Be surface enriched with D will enhance the sputtering yield as will be discussed in section 3.2. The good agreement between set III and the simulated values is therefore also explained, since a high initial D content together with a low D flux can be compared to a high D flux like the one in the simulations.

We also add the 100 eV result of another MD simulation study by Ueda *et al* [44], in which a simple two-body potential was used for Be–Be interactions and Be–H interactions were modelled with a combined Tersoff [33] and two-body potential. This single point, shown as a grey diamond in figure 1, agrees with our simulated values.

The line in the graph represents the Eckstein formula [42, 45] with parameter values as given in [45]. It is seen to match the simulated yields well, although at 7–10 eV, the simulated values are slightly higher. The Eckstein formula includes only physical sputtering, whereas the simulations predicts some chemical effects as discussed below.

As concluding remarks for the comparison of total sputtering yield, we simply state that the different experimental conditions when compared to the simulated ones make a straightforward comparison difficult. Firstly, the experimental samples can differ greatly from the simulated samples, since they are polycrystalline, may contain impurities and have some amount of impurities at the surface. Secondly, temperature driven effects (e.g. diffusion) are also a factor,

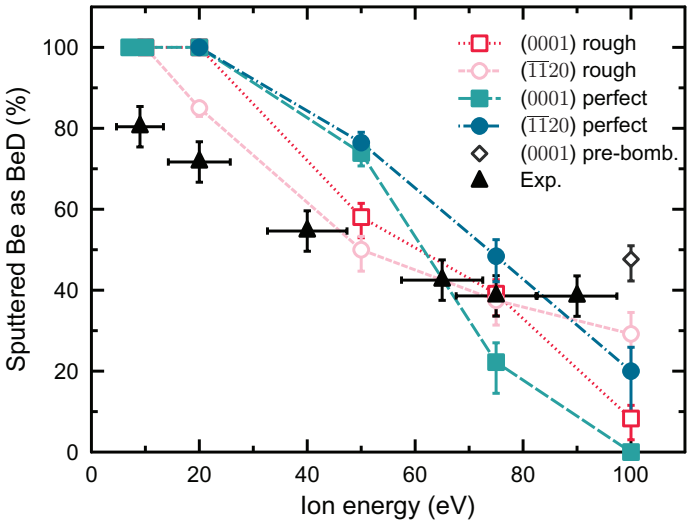

Figure 2. Fraction of Be atoms sputtered as BeD molecules after Be exposure to a D plasma. Both simulated and experimental data are shown. Two different orientations of the Be surface and both initially rough and perfect surfaces were used in the simulations.

since the short-time simulations are incapable of modelling these. Even so, keeping this in mind, the above comparisons can help in gaining understanding of the sputtering process.

3.1.2. Molecule fraction. The fraction of Be atoms that are sputtered as BeD molecules in the simulations and experiments in this work is plotted in figure 2. At low energies, the simulated fraction is about 100% for almost all surfaces in the simulation, meaning that no single Be atoms are sputtered. At higher energies the BeD fraction is smaller. The same trend is seen in the experiments, with the fraction going from about 80% at low energies to about 40% at energies above 70 eV. The fraction for the pre-bombarded sample at 100 eV is about 45%.

A closer look at the BeD sputter cases revealed that it is not the incoming D ion that forms the sputtered BeD molecule, but rather a D atom that is initially bound to the Be atom. Among the sputtered species we also observed some BeD_2 molecules (about 10% of all BeD molecules), many D_2 molecules but only one Be_2 molecule. Unfortunately, we were not able to observe any BeD_2 molecules in the experiments, since the emission from these occurs in the infrared spectrum [46] and the experimental spectrometer presently used for these measurements is incapable of detecting such long wavelengths.

3.2. The sputtering mechanism

The maximum transferable energy $T_{\max}$, in a collision between an energetic ion of mass M_1 and with an energy E_1 and a substrate atom of mass M_2 is [39]

$$T_{\max} = \frac{4M_1M_2}{(M_1+M_2)^2}E_1. \tag{2}$$

Therefore, a 7 eV D ion can at most give ∼4 eV to a beryllium atom in one collision. If an atom is to be physically sputtered, it has to receive an energy component normal to the surface and

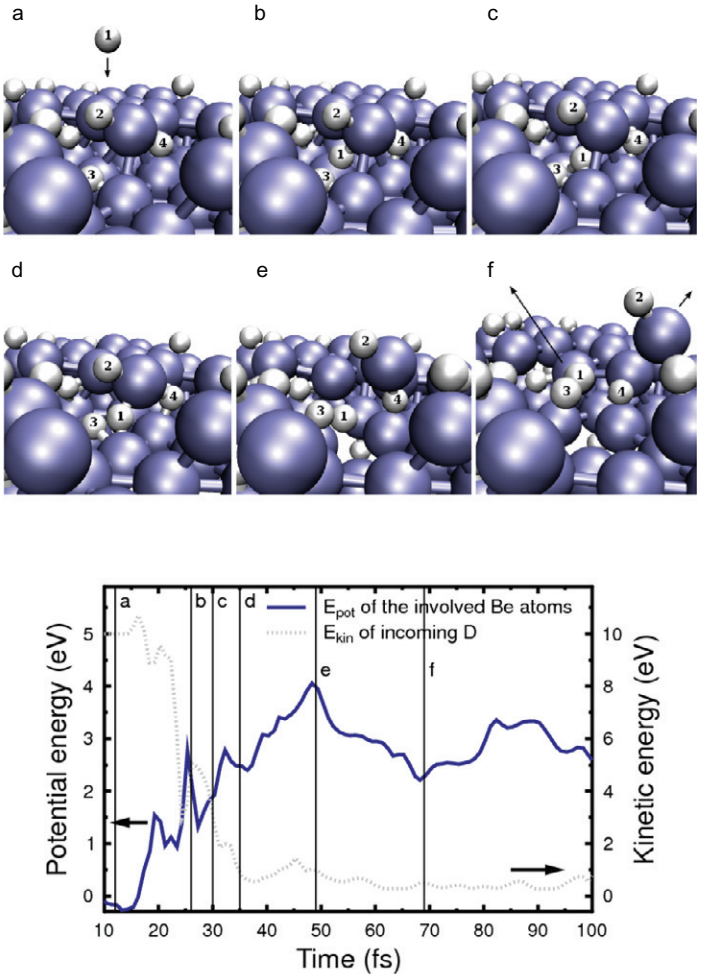

Figure 3. An illustration of a sputtering event. The upper part of the figure shows snapshots of the situation at six different times during the process. The D ions are represented by the small light grey spheres and the Be atoms are the larger dark spheres. The graph in the lower part illustrates the kinetic energy of the incoming D ion (dotted line) and the potential energy of the Be atoms that are initially bonded with the sputtered Be atom (solid line). The initial potential energy of these is chosen as zero level energy. The times corresponding to the snapshots are indicated with vertical lines in the graph and the arrows in the last snapshot (f) show in which direction the sputtered D_2 and BeD molecules are moving.

directed upwards, that is equal to the surface threshold energy. This energy was calculated to be $\gtrsim$6 eV for the Be surfaces at 320 K within this potential. Therefore, it is highly unlikely that a Be atom receives the necessary energy for physical sputtering during bombardment of 7–10 eV D ions at normal incidence, which implies that another sputtering mechanism is involved in the erosion at this energy.

To identify this mechanism, the energetics of the involved atoms was examined and the movement of the atoms during the sputtering processes was visually inspected. One sputtering case where a 10 eV D ion is bombarding a (0001) rough surface, is shown in figure 3. The graph illustrates both the potential energy of all Be atoms initially within the potential cutoff (2.9 Å)

to the sputtered Be atom and the kinetic energy of the incoming D ion. In the upper part of the figure, the sputtering process is illustrated with snapshots of the situation at six different times, labelled a–f. The corresponding times are indicated with vertical lines in the energy graph.

The behaviour of the kinetic energy of the incoming ion (labelled 1 in the snapshots) indicates that it loses energy in at least three events, which is seen as drops in the graph at about 17, 24 and 30 fs. The peaks in the curve show an increase in energy when it is drawn towards a Be atom due to attractive forces. At the end, the D ion is sputtered away as part of a D_2 molecule and it has lost more than 90% of its initial kinetic energy.

A loss of energy of the D ion is a gain in potential energy of the Be atoms. Between times *a* and *b*, the D collides with a Be atom, losing about 6 eV in the process. The rest of its kinetic energy is lost when it penetrates in between the Be atoms in *c*–*e*. In total, the D ion has caused five Be–Be bonds to be broken. Initially, four D ions were neighbours to the sputtered Be, but only one of these, number 2 in the snapshots, was sputtered with the Be. (Here, an atom being inside the cutoff range of the potential is considered as a neighbour.)

After time *b* (26 fs) the D ion has about 5 eV of kinetic energy. The soon-to-be-sputtered Be atom has now still got three bonds to the surface atoms, but has received enough kinetic energy to escape.

In a few cases the incoming D ion collided with a D atom already present in the lattice, which was thereafter able to break Be–Be bonds and cause sputtering.

The fact that a 7 eV D ion is able to sputter a Be atom indicates that the Be atom is weakly bonded to the surface. The fewer bonds it has to the other surface Be atoms, the weaker the binding is. The energy per bond for a surface Be atom with nine Be neighbours was estimated to be, on average, 0.30 ± 0.01 eV and with six Be neighbours 0.36 ± 0.02 eV. Calculating the same energies when a few D bonds are present resulted in: nine Be and two D bonds $= 0.25 \pm 0.01$ eV and six Be and three D bonds $= 0.28 \pm 0.02$ eV.

An analysis of the initial neighbours to the sputtered Be atom reveals that at low energies, the amount of Be neighbours is less than the amount in high-energy cases where it reaches the ideal one of nine of a hcp (0001) surface (see figure 4). The amount of D neighbours shows the opposite trend due to larger penetration depths of the D ions at higher energies.

The D atoms at the surface weaken the surface binding of Be atoms, making them easier targets for sputtering. If an incoming ion then enters the region between the surface Be and its neighbouring Be (as in figure 3), and in that way breaks their bonds, it loosens the Be atom's binding further and it can easily be sputtered away with one (or more) of its D neighbours to form a BeD molecule. This swift chemical sputtering (SCS) mechanism has been observed in covalently bonded material, like C and hydrogenated amorphous Si [9], but not previously in metals.

Nordlund *et al* [9] state that 'the SCS mechanism cannot happen in appreciable amounts in metals, since it requires the presence of loosely bound atoms or molecules at the surface, that are only bound to the substrate by one or at most a few chemical bonds'. This study shows that the mechanism can indeed be important in metals if the surface atoms for some reason have a weakened bond to the surface. The weakening can, as in this case, be due to roughening of the surface due to prolonged bombardment in combination with binding to D atoms.

Moreover, while it is well known that molecules can sputter from heat spikes [47, 48], these cannot be formed by the current very low energy and light ion irradiation of a low atomic mass target [49, 50]. Molecular sputtering for conditions outside the heat spike regime, as in this case, has been believed to occur only for molecular materials [20].

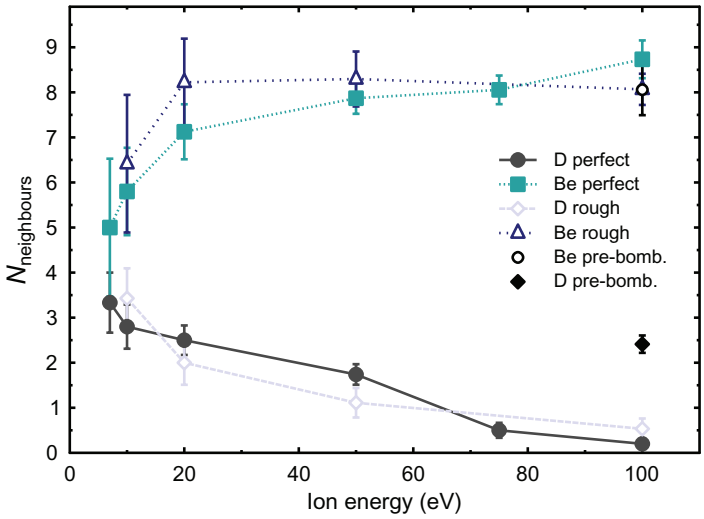

Figure 4. Average number and type of initial neighbours of the sputtered Be atoms. The data are from bombardment of a perfect and a rough Be (0001) surface.

The same initial neighbour analysis as in figure 4 for the experimental case would result in different values especially at high energies. This is because, as previously mentioned, during the measurements, even if bombarding a sample with 100 eV ions, there are always low-energy neutral atoms and molecules adsorbing on the surface. Therefore, there is a higher possibility that a surface Be atom has D neighbours when comparing to the situation in the simulations where all incoming particles have an energy of 100 eV, and will most likely penetrate into the sample. This is also consistent with the higher experimental fraction of sputtered BeD molecules at high energies (see figure 2), since D neighbours to Be atoms weaken the Be bond to the surface, as explained above. Indeed, using a pre-bombarded surface (hence having D atoms at the surface) in 100 eV bombardment simulations resulted in a similar fraction as in the experiments.

We note that the concept of bond breaking is not straightforwardly applicable to metals as it is in covalent materials, since the binding is here between the electron cloud and the metal ions. With the potential used in this work, the cohesive energy of an atom is dependent on the neighbouring atoms, i.e. on the amount and directions of atom bonds (see equation (1)), and every bond can be assigned an energy. This approach, however, shown to be consistent with the second moment tight-binding approximation and embedded-atom methods commonly used to model metals and has, in addition to Be, also successfully been applied to e.g. Fe [35], W [36] and Pt [34].

4. Conclusions

In this work, the experimental observation that BeD molecules are sputtered when Be is exposed to a D plasma was explained. It was shown that the swift chemical sputtering mechanism, previously considered to be important only in covalently bonded materials, must also be taken into account in metals. The chemical effects are considerable, since the simulations show that 100% of the sputtered Be atoms come out in BeD molecules at low (7–20 eV) ion energies, and

the experimental fraction was seen to decrease from about 80 to 40% over the 9–90 eV energy range. This ion energy dependence was ascribed to changes in the amount of D neighbours to surface Be atoms. This, in turn, is due to larger penetration depths of the D ions at high energies.

Acknowledgments

This work was performed within the Finnish Centre of Excellence in Computational Molecular Science (CMS), financed by The Academy of Finland and the University of Helsinki. It was also supported by the European Community under the contract of Association between Euratom/Tekes, and carried out within the framework of the European Fusion Development Agreement. The views and opinions expressed herein do not necessarily reflect those of the European Commission.

References

[1] Behrisch R (ed) 1981 *Sputtering by Particle Bombardment I* (Berlin: Springer)
[2] Sigmund P 1993 Introduction to sputtering *Mat.-Fys. Medd. K. Dan. Vidensk. Selsk.* **43** 7–26
[3] Erlebacher J, Aziz M J, Chason E, Sinclair M B and Floro J A 1999 Spontaneous pattern formation on ion bombarded si(001) *Phys. Rev. Lett.* **82** 2330
[4] Norris S A, Brenner M P and Aziz M J 2009 From crater functions to partial differential equations: a new approach to ion bombardment induced nonequilibrium pattern formation *J. Phys.: Condens. Matter* **21** 224017
[5] Schiller S, Goedicke K, Reschke J, Kirchhoff V, Schneider S and Milde F 1993 Pulsed magnetron sputter technology *Surf. Coat. Technol.* **61** 331–7
[6] Kellermann G and Craievich A F 2002 Structure and melting of bi nanocrystals embedded in a B_2O_3–Na_2O glass *Phys. Rev.* B **65** 134204
[7] Benninghoven A, Rudenauer F G and Werner H W 1987 *Secondary Ion Mass Spectrometry: Basic Concepts, Instrumental Aspects, Applications and Trends* (New York: Wiley)
[8] Samela J and Nordlund K 2007 Dynamics of cluster induced sputtering in gold *Nucl. Instrum. Methods Phys. Res.* B **263** 375
[9] Nordlund K, Salonen E, Krasheninnikov A V and Keinonen J 2006 Swift chemical sputtering of covalently bonded materials *Pure Appl. Chem.* **78** 1203–12
[10] Küppers J 1995 The hydrogen surface chemistry of carbon as a plasma facing material *Surf. Sci. Rep.* **22** 249–321
[11] Graves D B 1994 Plasma processing *IEEE Trans. Plasma Sci.* **22** 31–42
[12] Kleyn A W, Lopez Cardazo N J and Samm U 2006 Plasma–surface interaction in the context of ITER *Phys. Chem. Chem. Phys.* **8** 1761–74
[13] Janeschitz G 2001 ITER JCT and HTs. Plasma–wall interaction issues in ITER *J. Nucl. Mater.* **290–293** 1–11
[14] Salonen E, Nordlund K, Tarus J, Ahlgren T, Keinonen J and Wu C H 1999 Suppression of carbon erosion by hydrogen shielding during high-flux hydrogen bombardment *Phys. Rev. B (Rapid Comm.)* **60** 14005
[15] Salonen E, Nordlund K, Keinonen J and Wu C H 2001 Swift chemical sputtering of amorphous hydrogenated carbon *Phys. Rev.* B **63** 195415
[16] de Juan Pardo E, Balden M, Cieciwa B, Garcia-Rosales C and Roth J 2004 Erosion processes of carbon materials under hydrogen bombardment and their mitigation by doping *Phys. Scr.* **T111** 62–7
[17] Krstic P S, Reinhold C O and Stuart S 2007 Chemical sputtering from amorphous carbon under bombardment by deuterium atoms and molecules *New J. Phys.* **9** 209

[18] Meyer F W, Krstic P S, Vergara L I, Krause H F, Reinhold C O and Stuart S J 2007 Low energy chemical sputtering of ATJ graphite by atomic and molecular deuterium ions *Phys. Scr.* **T128** 50
[19] Roth J 1999 Chemical erosion of carbon based materials in fusion devices *J. Nucl. Mater.* **266–269** 51–7
[20] Johnson R E and Schou J 1993 Sputtering of inorganic insulators *Mat.-Fys. Medd. K. Dan. Vidensk. Selsk.* **43** 403–93
[21] ITER Physics Basis Editors and Physics ITER Expert Group Chairs and Co-Chairs and Joint ITER Central Team and Physics Integration Unit 1999 ITER physics basis *Nucl. Fusion* **39** 2137–638
[22] Federici G 2006 Plasma wall interactions in ITER *Phys. Scr.* T **124** 1–8
[23] Doerner R P, Baldwin M, Hanna J, Linsmeier C, Nishijima D, Pugno R, Roth J, Schmid K and Wiltner A 2007 Interaction of beryllium containing plasma with ITER materials *Phys. Scr.* T **128** 115–20
[24] Causey R A 2002 Hydrogen isotope retention and recycling in fusion reactor plasma-facing components *J. Nucl. Mater.* **300** 91
[25] Duxbury G, Stamp M F and Summers H P 1998 Observations and modelling of diatomic molecular spectra from JET *Plasma Phys. Control. Fusion* **40** 361
[26] Doerner R P, Baldwin M J, Buchenauer D, De Temmerman G and Nishijima D 2009 The role of beryllium deuteride in plasma–beryllium interactions *J. Nucl. Mater.* **390–391** 681–4
[27] Nishijima D, Doerner R P, Baldwin M J, De Temmerman G and Hollmann E M 2008 Properties of bed molecules in edge plasma relevant conditions *Plasma Phys. Control. Fusion* **50** 125007
[28] Nishijima D, Doerner R P, Baldwin M J and De Temmerman G 2009 Erosion yields of deposited beryllium layers *J. Nucl. Mater.* **390–391** 132–5
[29] Goebel D M, Campbell G and Conn R W 1984 Plasma surface interaction experimental facility (PISCES) for materials and edge physics studies *J. Nucl. Mater.* **121** 277
[30] *ADAS User Manual* version 2.6 2004 http://adas.phys.strath.ac.uk
[31] Nordlund K 2006 PARCAS computer code
[32] Björkas C, Juslin N, Timko H, Vörtler K, Henriksson K and Erhart P 2009 Development of interatomic potentials for Be, Be-C and Be-H *J. Phys.: Condens. Matter* **21** 445002
[33] Tersoff J 1988 New empirical approach for the structure and energy of covalent systems *Phys. Rev.* B **37** 6991
[34] Albe K, Nordlund K and Averback R S 2002 Modeling metal–semiconductor interaction: analytical bond-order potential for platinum–carbon *Phys. Rev.* B **65** 195124
[35] Müller M, Erhart P and Albe K 2007 Analytic bond-order potential for bcc and fcc iron—comparison with established embedded-atom method potentials *J. Phys.: Condens. Matter* **19** 326220
[36] Juslin N, Erhart P, Träskelin P, Nord J, Henriksson K O E, Nordlund K, Salonen E and Albe K 2005 Analytical interatomic potential for modelling non-equilibrium processes in the W–C–H system *J. Appl. Phys.* **98** 123520
[37] Brenner D W 1990 Empirical potential for hydrocarbons for use in simulating the chemical vapor deposition of diamond films *Phys. Rev.* B **42** 9458
[38] Berendsen H J C, Postma J P M, van Gunsteren W F, DiNola A and Haak J R 1984 Molecular dynamics with coupling to external bath *J. Chem. Phys.* **81** 3684
[39] Ziegler J F, Biersack J P and Littmark U 1985 *The Stopping and Range of Ions in Matter* (New York: Pergamon)
[40] le Page J, Mason D R, Race C P and Foulkes W M C 2009 How good is damped molecular dynamics as a method to simulate radiation damage in metals? *New J. Phys.* **11** 013004
[41] Roth J, Eckstein W and Guseva M 1997 Erosion of Be as plasma-facing material *Fusion Eng. Des.* **37** 465–80
[42] Eckstein W and Preuss R 2003 New fit formulae for the sputtering yield *J. Nucl. Mater.* **320** 209–13
[43] Doerner R P, Grossman A, Luckhardt S, Seraydarian R, Sze F C, Whyte D G and Conn R W 1997 Response of beryllium to deuterium plasma bombardment *J. Nucl. Mater.* **257** 51–8
[44] Ueda S, Ohsaka T and Kuwajima S 1998 Sputtering studies od beryllium with helium and deuterium using molecular dynamics simulations *J. Nucl. Mater.* **283–287** 1100–4
[45] Behrisch R and Eckstein W (ed) 2007 *Sputtering by Particle Bombardment: Experiments and Computer Calculations from Threshold to Mev Energies* (Berlin: Springer)

[46] Tereszchuk K, Bernath P F, Shayesteh A and Colin R 2002 The vibration–rotation emission spectrum of free BeH_2 *Science* **297** 1323
[47] Wucher A, Wahl M and Oechsner H 1993 Sputtered neutral silver clusters up to Ag_{18} *Nucl. Instrum. Methods Phys. Rev.* B **82** 337–46
[48] Henriksson K O E, Nordlund K and Keinonen J 2005 Fragmentation of sputtered silver and gold clusters *Phys. Rev.* B **71** 014117
[49] Thompson D A 1981 High density cascade effects *Rad. Eff.* **56** 105 and references therein
[50] Averback R S and Diaz de la Rubia T 1998 Displacement damage in irradiated metals and semiconductors *Solid State Physics* vol 51 ed H Ehrenfest and F Spaepen (New York: Academic) pp 281–402
[51] Nordlund K, Ghaly M, Averback R S, Caturla M, Diaz de la Rubia T and Tarus J 1998 Defect production in collision cascades in elemental semiconductors and fcc metals *Phys. Rev.* B **57** 7556–70
[52] Ghaly M, Nordlund K and Averback R S 1999 Molecular dynamics investigations of surface damage produced by keV self-bombardment of solids *Phil. Mag.* A **79** 795
[53] Nordlund K 1995 Molecular dynamics simulation of ion ranges in the 1–100 keV energy range *Comput. Mater. Sci.* **3** 448